DOI: 10.1002/ejoc.200901135

Molecular Rotors Based on the Boron Dipyrromethene Fluorophore

Andrew C. Benniston,[a] Anthony Harriman,*[a] Victoria L. Whittle,[a] and Mischa Zelzer[a]

Keywords: Dyes/pigments / Fluorescence / Viscosity / Sensors / Photophysics

In order to examine how changes in the size of the rotary group affect the efficacy of molecular probes for monitoring changes in local viscosity, a boron dipyrromethene dye bearing a *meso*-phenanthrene unit has been synthesized and fully characterized. ^{19}F NMR spectroscopy, together with molecular modelling, indicates that the bulky phenanthryl unit cannot rotate completely around the connecting C–C linkage but can oscillate over a reasonably large dihedral angle. This situation is to be contrasted with the corresponding dye having a *meso*-phenylene ring. The latter dye functions as a molecular probe for changes in viscosity of the surrounding solvent but remains essentially insensitive to changes in the polarity of the solvent. The opposite situation is found for the phenanthryl derivative, where a charge-transfer state lies at higher energy than the emissive π,π^* excited state but can be accessed thermally. The results are considered in terms of energy-level diagrams taking into account rotational freedom. Photophysical properties are reported for both dyes in a range of solvents, and temperature-dependent studies are described.

Introduction

Numerous fluorescent rotors have been reported that can be used to monitor changes in local viscosity and/or flow rate.[1] A common feature of all such compounds relates to the coupling of some type of mechanical motion of a particular subunit with nonradiative deactivation of the excited singlet state. It is in this manner that the fluorescence yield and lifetime increase with increasing frictional forces between the rotor and the surrounding solvent molecules.[2] The actual mechanism by which mechanical operation of the rotor leads to enhanced nonradiative decay of the fluorescent state is not always easily understood but often involves charge-transfer interactions. Because of this latter behaviour, the rotor might respond to changes in local polarity as well as perturbations of the surrounding rheology.[3] Furthermore, different types of rotors show disparate sensitivity towards changes in local viscosity and are susceptible to specific solvent effects.[4] Calibration of the system can be hazardous in such cases. Nonetheless, the use of fluorescent rotors to probe environmental effects in microporous media,[5] intact biological cells,[6] highly toxic conditions,[7] unusual liquids[8] or within lipid membranes[9] is a rapidly expanding topic with significant industrial applications.

Although numerous types of fluorophores have been proposed, boron dipyrromethene (Bodipy) dyes have several important advantages in the field of molecular rotors, and some key prototypes have been advanced.[10] The most promising Bodipy-based systems are designed with the rotor being attached at the *meso* position of the dipyrrin backbone but with the latter lacking the usual alkyl substituents from the pyrrole ring.[11] This simple strategy allows restricted rotation of the rotor in the ground state, which otherwise is blocked by steric hindrance with the alkyl groups. Mechanistic studies have shown that gyration of the rotor involves concerted distortion of the dipyrrin backbone,[11,12] and it is this nuclear twisting that leads to enhanced nonradiative decay. To-date, studies have been restricted to Bodipy-based dyes equipped only with a *meso*-phenylene ring (PHBOD) as the rotor, although this is usually substituted with a long alkyl chain to facilitate incorporation into biological media. We hereby introduce a new Bodipy-based molecular rotor where the phenylene ring is replaced with a 9-phenanthrene unit (PHENBOD) and compare the properties of the two compounds. It will be shown that this simple replacement causes major changes in the sensory activities of the probe.

[a] Molecular Photonics Laboratory, School of Chemistry, Bedson Building, Newcastle University,
Newcastle upon Tyne NE1 7RU, United Kingdom
Fax: +44-191-222-8660
E-mail: anthony.harriman@ncl.ac.uk

Results and Discussion

Synthesis and ^{19}F NMR Spectroscopy

Outlined in Scheme 1 are the synthetic procedures used to prepare the dyad PHENBOD. Reaction of phenanthrene-9-carbaldehyde with excess pyrrole produced, after careful chromatography, the intermediate **1** in 54% yield. Oxidation of **1** with DDQ followed by chelation to the BF_2 unit formed the desired rotor PHENBOD as a red solid. The authenticity and purity of the product was

proven by standard analytical techniques, including mass spectrometry, ^{1}H, ^{13}C, ^{19}F and ^{11}B NMR spectroscopy, melting point and elemental analysis. The putative rotor is soluble in most organic solvents, but is quite insoluble in water.

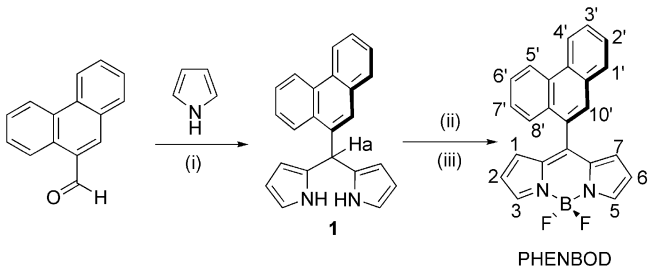

Scheme 1. Reagents and conditions: (i) CF_3CO_2H, room temperature, 90 h; (ii) DDQ; (iii) *N*,*N*-diisopropylethylamine, $BF_3{\cdot}Et_2O$. The atomic numbering scheme is also shown.

Owing to the low symmetry of PHENBOD, the two fluorine atoms are inequivalent in NMR terms for all non-planar rotamers. One break from this rule is the all-planar conformer, but this is highly unfavourable because of severe steric clashes between the 1,7-dipyrrin hydrogen atoms and protons at the 8,10-positions of the phenanthrene nucleus (Figure 1). Semiempirical molecular modelling of the rotor is in full agreement with this notion; the torsion angle between the phenanthrene and dipyrrin residues being 60°. Evidently, if the phenanthrene were free to rotate, the lack of equivalency of the two fluorine atoms would be relaxed since the sites would readily interchange. It turns out that ^{19}F NMR spectroscopy is an especially adept tool by which to distinguish disparate fluorine chemical environments, and provides direct evidence of fluxional processes. Generally, for symmetrical Bodipy compounds the ^{19}F NMR spectrum consists of a single quartet, due to the two equivalent fluorine atoms coupling to the single ^{11}B (I = 3/2) nucleus. That the ^{19}F NMR spectrum recorded for PHENBOD in $CDCl_3$ consists of 16 lines, with minor satellite peaks, is clear indication that the fluorine atoms reside in different environments, and moreover stipulates that the phenanthrene gyration rate is slow on the NMR timescale. It is possible to simulate the spectrum as two chemically inequivalent fluorine atoms coupling to the major ^{11}B (80.4%) and minor ^{10}B (19.6%) nuclei.

Variable-temperature ^{19}F NMR spectra recorded for PHENBOD in [D_6]DMSO (DMSO = dimethyl sulfoxide) afforded more insight into the phenanthrene rotation dynamics. Thus, the room-temperature spectrum (Figure 1) is dominated by two well-separated resonances ($\Delta\delta$ = 0.9 ppm) that are modelled adequately as two inequivalent fluorine atoms. The significant $\Delta\delta$ value implies that F_a and F_b reside in different chemical environments, and are shielded (or deshielded) by the proximal phenanthrene unit. Except for recognized solvent-induced chemical shifts,[13] the ^{19}F NMR spectrum recorded at 323 K is identical to that shown in Figure 1. Even at 393 K (i.e., the maximum temperature attained), there is no evidence of the peaks coalescing. On the basis of these findings, we conclude that

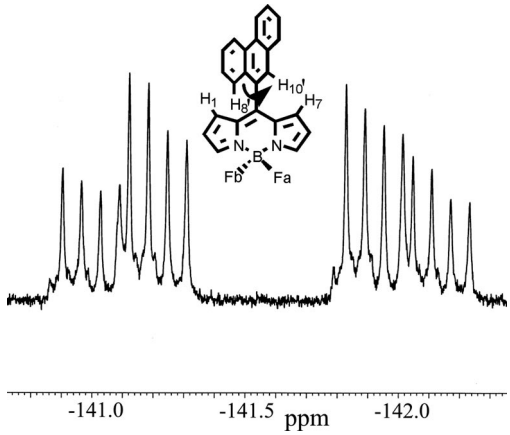

Figure 1. Room-temperature ^{19}F NMR spectrum recorded for PHENBOD in [D_6]DMSO. The formula shows the partial proton-numbering scheme. Note: the minor resonances arise from coupling of the fluorine atoms to the ^{10}B nucleus.

the rate of gyration of the phenanthrene unit at room temperature must be significantly less than 1 Hz. The more likely scenario, therefore, is that the phenanthrene residue acts as a "flipper" and alternates between the two extreme torsion angles. This oscillatory motion is likely to be fast on the NMR timescale, and could lead to transient distortion of the Bodipy group as the phenanthrene and dipyrrin units attempt to become co-planar.

Electrochemistry

The electrochemical properties of the two dyes were studied by cyclic voltammetry in CH_2Cl_2 containing a background electrolyte. For PHBOD, a quasi-reversible reduction peak is seen on cathodic scans that correspond to a half-wave potential ($E_{1/2}$) of –0.68 V vs. SCE, with a peak separation of 90 mV. This process is assigned to the one-electron reduction of the Bodipy nucleus on the basis of earlier studies made with related compounds.[14] For PHENBOD under identical conditions, $E_{1/2}$ has a value of –0.70 V vs. SCE, again with a peak separation of 90 mV. Thus, increasing the size of the *meso* substituent has no obvious effect of reduction of the Bodipy unit to the corresponding π-radical anion. No reduction wave is seen that could be attributed to reduction of the phenanthrene residue.

On anodic scans, PHBOD shows a single, irreversible peak centred at 1.75 V vs. SCE that can be assigned to the one-electron oxidation of the Bodipy core. The irreversible character of this wave is a known characteristic of removing the alkyl substituents from the dipyrrin framework.[15] No additional peaks are seen in the cyclic voltammograms recorded for PHBOD, regardless of scan rate or solvent. However, PHENBOD exhibits two irreversible oxidation peaks in CH_2Cl_2 solution. The first peak is centred at 1.69 V vs. SCE and is assigned to the one-electron oxidation of the Bodipy nucleus.[14] The second peak occurs at 1.87 V vs. SCE and can be attributed to a one-electron oxidation

of the *meso*-phenanthrene unit. Although electrochemically irreversible, these electrochemical data can be used in conjunction with the optical spectroscopic data (see below) to conclude that there are no accessible intramolecular light-induced, electron-transfer reactions open to PHBOD. For PHENBOD, there is likely to be an intramolecular charge-transfer state (CTS) situated at somewhat higher energy than the first excited singlet (S_1) state localized on the Bodipy core. It is difficult to predict the actual energy of this CTS, because of the irreversible nature of the oxidative electrochemistry, but it will be less than 200 meV above that of the S_1 state in CH_2Cl_2 solution. Furthermore, its energy is likely to be affected by changes in the solvent polarity.

Photophysical Properties of PHBOD

Photophysical data for PHBOD in both toluene solution and a plastic film have been reported previously,[11,12] and only new information is presented here. For comparative purposes, the absorption maximum (λ_{MAX} = 501 nm) and fluorescence peak (λ_{FLU} = 517 nm) measured in toluene at room temperature are as reported before, whereas the fluorescence quantum yield (Φ_F = 0.052) and emission lifetime (τ_S = 0.44 ns) remain comparable to the literature values.[12] Time-resolved fluorescence decay curves are strictly mono-exponential, whereas there is excellent agreement between absorption spectra and corrected excitation spectra across the visible region. The radiative rate constant ($k_{RAD} = \Phi_F/\tau_S$) is in good agreement with that calculated from the Strickler–Berg expression[16] but both Φ_F and τ_S are much lower than found for analogous Bodipy dyes bearing alkyl groups on the dipyrrin framework.[17] This situation points towards an enhanced rate constant [$k_{NR} = (1 - \Phi_F)/\tau_S$] for nonradiative decay of the S_1 state due to the so-called rotor effect.

Additional studies were made to examine the effect of solvent viscosity (η) on k_{NR} for PHBOD at 20 °C, and the results are given in Table 1. The solvents used were a series of linear *n*-alkanols together with selected solvents needed to distinguish between viscosity and polarity effects, the latter being expressed in terms of the static dielectric constant (ε_S). Throughout this set of solvents, both λ_{MAX} and λ_{FLU} show a small dependence on the polarizability of the medium,[18] as is normal behaviour for Bodipy dyes.[19] More significantly, k_{NR} decreases progressively with increasing viscosity but shows much less correlation with the polarity of the solvent. Indeed, there is a reasonably good fit to Equation (1) (Figure 2), where υ is a limiting pressure, a is a coefficient that effectively converts bulk viscosity to a type of micro-viscosity,[20] and E_A is the activation energy for the rotor effect.[11] The derived value for a (a = 0.31) is a key parameter for expressing the sensitivity of the fluorescent rotor towards changes in viscosity; the value found here indicates that PHBOD is a valuable, but rather less than perfect, probe for viscosity changes. An extremely important finding here is that earlier work with a closely related derivative of PHBOD having a long paraffinic chain at the 4-position of the *meso*-phenylene ring found a = 0.44.[11] The significance of this finding is that the sensitivity towards changes in viscosity can be tuned by modifying the nature of peripheral substituents, this being a simple synthetic operation.

$$k_{NR} = \frac{\upsilon}{\eta^{a}} e^{-\frac{E_A}{RT}} \quad (1)$$

Table 1. Photophysical properties recorded for PHBOD in selected solvents at 20 °C.

Solvent	η [cP]	ε_S	Φ_F	τ_S [ns]	k_{NR} [10^9 s^{-1}]
CH_3OH	0.54	32.6	0.035	0.29	3.33
C_2H_5OH	0.69	24.6	0.040	0.33	2.91
C_3H_7OH	1.95	20.1	0.046	0.39	2.45
C_4H_9OH	2.54	17.8	0.061	0.53	1.77
$C_5H_{11}OH$	3.62	15.1	0.068	0.57	1.64
$C_6H_{13}OH$	4.58	13.3	0.074	0.61	1.52
$C_7H_{15}OH$	5.81	11.9	0.078	0.63	1.46
$C_8H_{17}OH$	7.29	10.3	0.090	0.76	1.20
$C_9H_{19}OH$	9.15	–	0.098	0.81	1.11
$C_{10}H_{21}OH$	10.9	7.9	0.105	0.84	1.07
CHX[a]	0.63	2.0	0.039	0.33	2.91
DCE[b]	0.78	10.4	0.041	0.40	2.40
THF[c]	0.46	7.5	0.030	0.27	3.59
CH_3CN	0.37	36.6	0.018	0.25	3.93
DMF[d]	0.79	38.2	0.044	0.40	2.40
DMSO[e]	1.99	47.2	0.046	0.52	1.83
PC[f]	3.4	64.9	0.067	0.59	1.58
Triacetin	16.2	6.2	0.130	1.02	0.85
Formamide	2.4	109.5	0.042	0.51	1.88

[a] Cyclohexane. [b] 1,2-Dichloroethane. [c] Tetrahydrofuran. [d] Dimethylformamide. [e] Dimethyl sulfoxide. [f] Propylene carbonate.

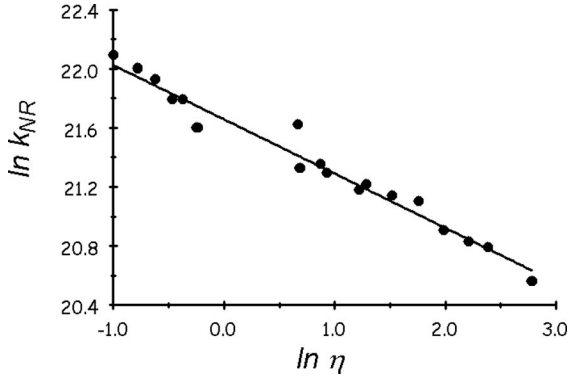

Figure 2. Effect of bulk viscosity on the rate constant for nonradiative decay of the S_1 state of PHBOD in solution at 20 °C. The solid line is a fit to Equation (1).

In ethanol solution, k_{NR} was found to exhibit a shallow dependence on temperature until approaching the freezing point of the solvent (Figure 3). As the solvent freezes, there is a dramatic fall in k_{NR} until reaching a lower limit in the resultant glassy matrix. At this point, Φ_F is close to unity and the rotary effect is switched off entirely. Temperature has but a small effect on the fluorescence spectral profile, with the band narrowing on freezing. In fluid solution, Arrhenius-like behaviour is not observed even over a small

temperature range. Correcting k_{NR} for the change in viscosity that accompanies cooling[21] improves the situation at the higher temperature range but still does not lead to a linear Arrhenius-type relationship over the whole region where the solvent is fluid. This situation can be used to argue that the rotational barrier is itself dependent on the viscosity; this could happen, for example, if ring rotation is a complex process having several transition states. In the high-temperature region, the barrier height at the S_1 level is only ca. 500 J mol^{-1}, which is much smaller than that found earlier for the long-chain analogue. The implication here is that interaction between the chain and the medium contributes towards the activation energy.

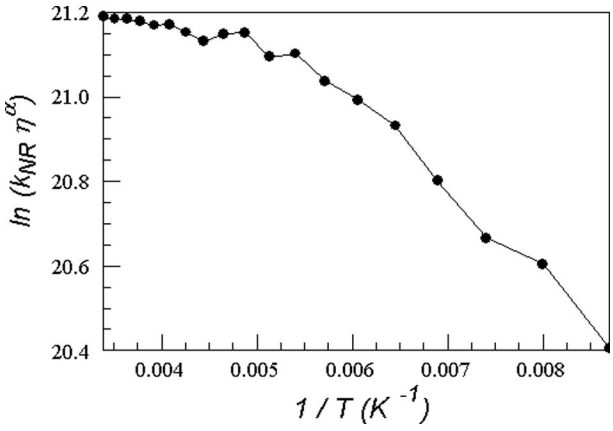

Figure 3. Arrhenius-type plot for the effect of temperature on the rate of nonradiative decay of the S_1 state for PHBOD in ethanol.

In the case of PHBOD the rotor effect corresponds to buckling of the dipyrrin backbone as the *meso*-phenylene rings rotates around the connecting C–C bond.[11,12] This introduces frictional forces with surrounding solvent molecules, but the relatively small value derived for α suggests that rotation occurs within a cavity that effectively screens the rotor from close interaction with the solvent. The barrier to ring rotation in the ground state, computed at the AM1 level, is ca. 46 kJ mol^{-1} and is in agreement with values calculated for related systems.[11,12] For the corresponding S_1 state the barrier is reduced considerably but, since the fluorescence spectrum and Stokes' shift are as expected for a sterically blocked Bodipy dye, it can be argued that emission occurs from a geometry similar to that of the ground state. Enhanced nonradiative decay to the ground state, therefore, can be explained within the confines of the pinhole-sink model[22] (Figure 4) where the potential energy surface for the S_1 state is somewhat porous. Leakage to the ground state can occur at specific geometries where the latter is unstable and, as a direct consequence, the rate is controlled by the energy-gap law.[23] As the energy gap decreases, there is a pronounced escalation in k_{NR}. It follows that the porosity of the upper surface, which sets the temperature dependence and viscosity sensitivity, is determined in part by the nature of any substituents attached to the *meso*-phenylene ring.

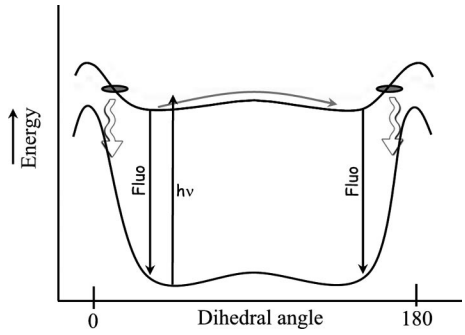

Figure 4. Potential energy diagram proposed to explain the behavior of PHBOD in a fluid solvent. The key feature is a flattened surface for the S_1 state that contains drain holes for coupling to the ground-state surface.

Photophysical Properties Recorded for PHENBOD

Turning attention now to PHENBOD, we note that the absorption and fluorescence spectra (Figure 5) remain unchanged from those recorded for PHBOD, with only a small spectral shift in solvents of differing polarizability.[18] In fluid solution at 20 °C, PHENBOD fluoresces with a small Stokes' shift (i.e., ca. 550 cm^{-1}), indicating that no substantial structural changes accompany excitation. Again, there is excellent agreement between absorption and excitation spectra across the visible and near-UV regions. The observed emission spectrum shows good mirror symmetry with the lowest energy-absorption band, and there are no additional features apparent in the emission spectrum compared to PHBOD. Pronounced differences are seen, however, in the photophysical properties recorded in different solvents at 20 °C (Table 2). Interestingly, any correlation between k_{NR} and bulk viscosity is far from obvious. Thus, increasing the size of the rotor has dampened out the ability to respond to changes in the viscosity of the surroundings, and this finding would appear to be in general accord with the idea that the *meso*-phenanthrene unit does not rotate fully around its connection. In particular, it is notable that, except in nonpolar solvents, Φ_F and τ_S recorded for PHENBOD greatly exceed those measured for PHBOD under identical conditions. For example, at room temperature in toluene Φ_F = 0.62 and τ_S = 4.9 ns; which represents a ten-fold increase in fluorescence yield and lifetime with respect to PHBOD.

As shown in Figure 6, for PHENBOD there is a reasonably clear correlation between k_{NR} and the static dielectric constant (ε_S) of the medium. This situation follows from the modest fall in both Φ_F and τ_S with increasing polarity of the solvent. For example, PHENBOD is highly fluorescent in butan-1-ol (Φ_F = 0.56; τ_S = 4.00), with the properties being similar to those of sterically hindered Bodipy dyes. In contrast, PHENBOD is weakly fluorescent in propylene carbonate solution (Φ_F = 0.30; τ_S = 2.10), despite the fact that the viscosities of these two solvents are similar and the realization that the values found for PHBOD remain the same in these solvents. The radiative rate constant is essentially insensitive to changes in the nature of the sol-

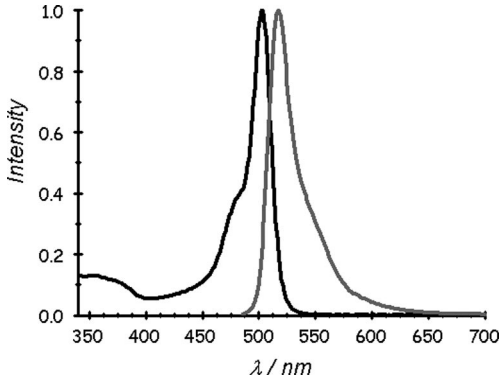

Figure 5. Absorption (black curve) and fluorescence (grey curve) spectra recorded for PHENBOD in methanol at room temperature.

Table 2. Photophysical properties recorded for PHENBOD in selected solvents at 20 °C.

Solvent	Φ_F	τ_S [ns]	k_{RAD} [10^8 s^{-1}]	k_{NR} [10^8 s^{-1}]
CH_3OH	0.40	2.75	1.45	1.89
C_2H_5OH	0.46	3.35	1.37	1.41
C_3H_7OH	0.54	3.88	1.39	1.19
C_4H_9OH	0.56	4.00	1.40	1.10
$C_5H_{11}OH$	0.57	4.08	1.40	1.05
$C_6H_{13}OH$	0.58	4.18	1.39	1.00
$C_7H_{15}OH$	0.60	4.27	1.41	0.94
$C_8H_{17}OH$	0.61	4.30	1.42	0.91
$C_9H_{19}OH$	0.62	4.38	1.42	0.87
$C_{10}H_{21}OH$	0.65	4.85	1.34	0.72
CHX[a]	0.68	4.95	1.37	0.65
DCE[b]	0.62	4.45	1.39	0.85
THF[c]	0.64	4.72	1.36	0.76
CH_3CN	0.57	4.05	1.41	1.85
DMF[d]	0.48	3.95	1.22	2.09
DMSO[e]	0.40	2.88	1.39	2.08
PC[f]	0.30	2.10	1.43	2.33
Triacetin	0.64	4.64	1.38	0.77
Formamide	0.19	1.28	1.48	2.66

[a] Cyclohexane. [b] 1,2-Dichloroethane. [c] Tetrahydrofuran. [d] Dimethylformamide. [e] Dimethyl sulfoxide. [f] Propylene carbonate.

vent; it is expected[24] to scale according to n^2 where n is the refractive index. Taking due account of the electrochemical data, it appears likely that there is a CTS accessible to PHENBOD that is unavailable to PHBOD and that the energy gap between S_1 and CTS is controlled by the solvent polarity. This hypothesis was explored by way of temperature-dependent fluorescence spectral studies.

The fluorescence yield and lifetime measured for PHENBOD in ethanol increase with decreasing temperature until reaching the glassy matrix, where the properties become independent of the temperature (Figure 7). Decreasing the temperature has no effect on the band shape or emission maximum until reaching the glassy region where the spectra sharpen but do not shift. The temperature effect on the corresponding k_{NR} values can be expressed in the form of Equation (2) where k_0 is the activationless rate constant for decay of the S_1 state. This latter term has a value of 3.7×10^7 s^{-1}. The activated rate constant, k_A, is calculated to be 8.3×10^{10} s^{-1}, whereas the activation barrier, E_A, is

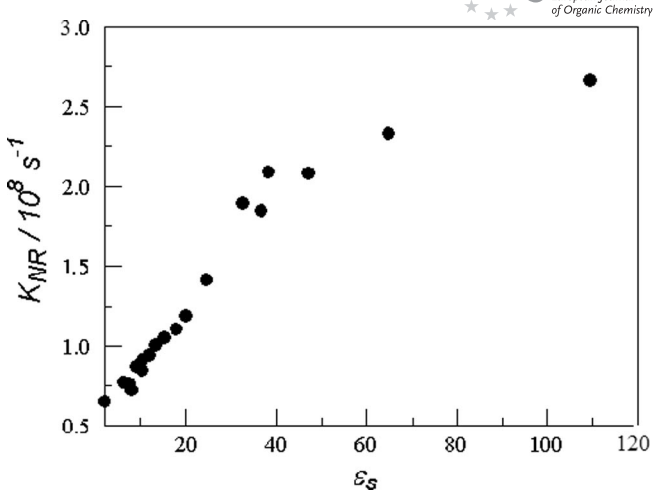

Figure 6. Effect of the solvent static dielectric constant on the rate constant for nonradiative decay of the S_1 state of PHENBOD, recorded at 20 °C.

found to be 16.5 kJ mol^{-1}. This barrier is associated with reaching the CTS from the S_1 state and is most likely controlled, at least in part, by the solvent polarity. Given that the CTS will possess a different geometry to that of the ground state, we might also expect that the barrier will con-

$$k = k_0 + k_1 e^{-\frac{E_A}{RT}} \quad (2)$$

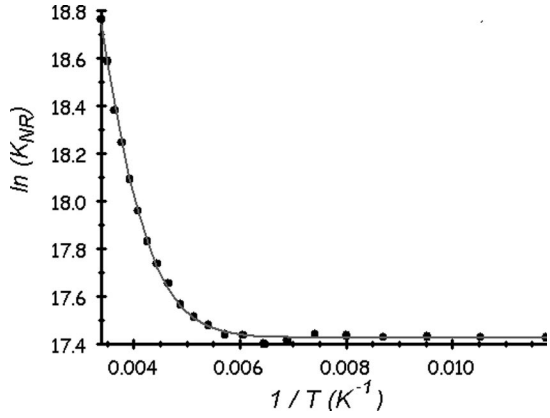

Figure 7. Arrhenius-type plot for the nonradiative decay of PHENBOD in ethanol. The solid line is a fit to Equation (2).

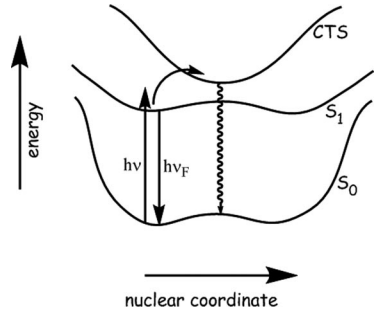

Figure 8. Proposed potential energy diagram accounting for the activated decay of the S_1 state for PHENBOD in a polar solvent.

tain a contribution from frictional forces with the surrounding solvent, and hence a modest dependence on the solvent viscosity. It is notable that there is no observable temperature dependence for the decay of the S_1 state in methylcyclohexane solution. The overall behaviour found for PHENBOD can now be expressed by way of Figure 8.

Conclusions

Replacing the *meso*-phenylene ring in PHBOD with a phenanthrene residue introduces a severe barrier to internal rotation to such a degree that the substituent cannot complete a full turn in the ground state. This is not too surprising, because even for PHBOD the dipyrrin backbone has to distort[11,12] in order to permit the phenyl ring to complete a full rotation. It is this structural distortion that leads to the so-called rotor effect. Simple oscillation of the substituent is insufficient to have much effect on k_{NR}. For the compound to function as an effective molecular rotor it then requires the excited-state potential surface to be adequately porous to couple the S_1 state to the ground state at sites other than the potential minima. This situation is described in Figure 4 and ensures that PHBOD acts as a fluorescent probe for changes in viscosity. The limiting factor controlling the performance of the probe can now be considered in terms of frictional forces between the rotor and surrounding solvent molecules. The rotational barrier is small, but finite, such that nonradiative decay occurs on the timescale of some hundreds of ps. This is very much slower than internal rotational times found for Rhodamine[25] and triphenylmethane[26] dyes and indicates the need for the dipyrrin framework to undergo a concerted distortion for rotation to occur. Improving the sensitivity of PHBOD as a viscosity probe requires an increase in the magnitude of these frictional forces but without curtailing rotation. This is best achieved by incorporating substituents at the top of the phenylene ring that will embed the rotor into the solvent structure. Indeed, it has already been concluded that such groups play a major role in setting the sensitivity of the rotor towards changes in viscosity and are also important in controlling the barrier height for ring rotation. Thus, next-generation rotors will be engineered with intelligent substituents built into the *meso* group.

The *meso* substituent present in PHENBOD cannot complete a full rotation in the ground state, but it can freely oscillate around the axis. This oscillation has little effect on the photophysical properties such that PHENBOD becomes a very poor probe for changes in viscosity. Even at the S_1 level, there is no inclination for full rotation, and there is no sign that the S_1 potential surface is porous. The implication of this finding is important for the rational design of advanced molecular rotors. In terms of Figure 4, the pinhole that allows coupling of the two surfaces appears to be sited near a co-planar geometry such that it is accessible to PHBOD but not to PHENBOD. This sink must take the form of an intramolecular vibration associated with twisting of the dipyrrin backbone.

However, a further consequence of using a fused polycycle as the rotary group is that the oxidation potential is significantly lower than that of a simple phenylene ring. For PHENBOD, an intramolecular CTS becomes thermally accessible to the S_1 state, especially in polar solvents where the energy of the CTS is lowered. The net result is a probe that shows a shallow response to solvent polarity but little sensitivity towards changes in viscosity. This effect can be further enhanced by replacing phenanthrene with 9-anthracene, which causes the energy of the CTS to become closely comparable with that of the S_1 state in polar solvents. At this point, normal fluorescence from the Bodipy dye is extinguished although the off-level is now set by weak charge-recombination emission. For PHENBOD in a polar solvent such as CH_3CN decay of the S_1 state results in partial formation of the corresponding triplet excited state. Indeed, the yield of the triplet state is significantly higher than that found in methylcyclohexane or for PHBOD in CH_3CN. It is possible, therefore, that triplet formation is a consequence of charge recombination within the CTS, as has been reported for other orthogonally positioned CTSs formed from molecular dyads.[27]

Experimental Section

General: Bulk chemicals were purchased at the highest purity available from Aldrich Chemical Co. and were used as received unless stated otherwise. Tetra-*n*-butylammonium tetrafluoroborate (TBATFB) from Fluka was recrystallized several times from methanol and dried thoroughly under vacuum before being stored in a desiccator. Standard solvents were dried by literature methods[28] before being distilled and stored under nitrogen over molecular sieves (4 Å). Spectroscopic grade solvents were used for all photophysical measurements. ^1H and ^{13}C NMR spectra were recorded with either Bruker Avance 300 MHz, JEOL 400 MHz, or JEOL Lambda 500 MHz spectrometers. ^{11}B and ^{19}F NMR spectra were recorded with the 400 MHz spectrometer. Variable-temperature ^{19}F NMR spectra were recorded with the 500 MHz spectrometer. Chemical shifts for ^1H and ^{13}C NMR spectra are referenced relative to the residual protiated solvent. The ^{11}B NMR chemical shift is referenced relative to $BF_3{\cdot}Et_2O$ (δ = 0 ppm), and the ^{19}F NMR chemical shift is given relative to $CFCl_3$ (δ = 0 ppm). Routine mass spectra and elemental analyses were obtained either by using in-house facilities or at Medac Ltd. Absorption spectra were recorded with a Hitachi U3310 spectrophotometer, and corrected fluorescence spectra were recorded with a Hitachi F-4500 spectrometer. Uncorrected melting points were measured with a Stuart SMP11 apparatus. Cyclic voltammetry experiments were performed with a fully automated HCH Instruments Electrochemical Analyzer and a three-electrode setup consisting of a platinum working electrode, a platinum wire counter electrode, and a silver wire reference electrode. Ferrocene was used an internal standard. All studies were performed in deoxygenated CH_2Cl_2 containing TBATFB (0.2 M) as background electrolyte. Solute concentrations were typically 0.1 mM. Redox potentials were reproducible to within ±15 mV. All luminescence measurements were made by using optically dilute solutions and were corrected for spectral imperfections of the instrument by reference to a standard lamp. Luminescence quantum yields were measured relative to a standard dye by using optically matched solutions.

Preparation of 1: A three-neck flask was charged with 9-phenanthrenecarboxaldehyde (2.06 g, 10 mmol) and evacuated and backfilled with nitrogen three times. Freshly distilled pyrrole (49.5 mL, 0.7 mol) was added and the solution purged with nitrogen in the dark for 1 h. Trifluoroacetic acid (0.077 mL, 1.0 mmol) was added dropwise to the reaction mixture, and the resultant blue/black solution was stirred at room temperature in the dark for 90 h. After confirmation by thin layer chromatography (aluminium oxide plate; petroleum ether/dichloromethane, 2:1) that the carboxaldehyde had been fully consumed, excess pyrrole was removed by vacuum distillation. The resultant blue/black residue was purified by flash column chromatography (basic activated aluminium oxide; petroleum ether/ethyl acetate, 4:1). After evaporation of the solvent, the yellow oily residue was dissolved in diethyl ether (5 × 20 mL) with the solvent being removed under reduced pressure after each addition. The solid was then washed with petroleum ether (2 × 5 mL) and dried under vacuum to give the desired product as a cream crystalline solid (1.76 g, 54%). ^{1}H NMR ($CDCl_3$, 300 MHz): δ = 8.74 (dd, ^3J = 7.5, ^4J = 0.9 Hz, 1 H, H$^{5'}$), 8.68 (d, ^3J = 8.1 Hz, 1 H, H$^{8'}$), 8.11 (dd, ^3J = 8.1, ^4J = 0.9 Hz, 1 H, H$^{4'}$), 7.97 (br. s, 2 H, NH), 7.76 (dd, ^3J = 7.8, ^4J = 1.2 Hz, 1 H, H$^{1'}$), 7.65 (ddd, ^3J = 7.5 and 6.9, ^4J = 1.5 Hz, 2 H, H$^{6'}$ and H$^{7'}$), 7.59–7.53 (m, 2 H, H$^{2'}$ and H$^{3'}$), 7.40 (s, 1 H, H$^{10'}$), 6.71 (dd, ^3J = 4.5, ^4J = 2.7 Hz, 2 H, H^3 and H^5), 6.28 (s, 1 H, H^a), 6.20 (dd, ^3J = 5.7, ^3J = 3.0 Hz, 2 H, H^2 and H^6) and 6.02 (dd, ^3J = 3.0, ^4J = 2.7 Hz, 2 H, H^1 and H^7) ppm. ^{13}C NMR ($CDCl_3$, 100 MHz): δ = 136.57 (1 C), 132.00 (1 C), 131.58 (1 C), 130.95 (1 C), 130.85 (1 C), 130.17 (1 C), 128.91 (1 C), 127.05 (1 C), 127.07 (1 C), 126.87 (1 C), 126.59 (2 C), 124.58 (1 C), 123.26 (1 C), 122.57 (1 C), 117.33 (1 C), 108.73 (1 C), 107.80 (1 C), 40.65 (1 C) ppm. TLC (aluminium oxide): R_f = 0.30 in petroleum ether/ethyl acetate, 4:1. M.p. 98–102 °C.

Preparation of PHENBOD: A three-neck flask was charged with **1** (1.62 g, 5.02 mmol) in freshly distilled CH_2Cl_2 (250 mL), and the solution was purged with nitrogen in the dark for 1 h. Dichlorodicyanobenzoquinone (3.42 g, 15.06 mmol) was added and the solution stirred at room temperature in the dark for 1.5 h. After confirmation by thin layer chromatography (silica gel plate, CH_2Cl_2) that all the dipyrromethane had been consumed, *N*,*N*-diisopropylethylamine (4.91 mL, 28.61 mmol) and boron trifluoride–diethyl ether (5.12 mL, 40.16 mmol) were added dropwise under nitrogen. The resultant dark brown solution was stirred in the dark for 20 h, until full consumption of the intermediate was confirmed by thin layer chromatography. The reaction mixture was subsequently diluted with additional CH_2Cl_2 (250 mL) and washed with brine (4 × 200 mL). The separated organic layer was dried with magnesium sulfate, filtered and the drying agent was washed thoroughly with CH_2Cl_2 (100 mL). The combined organic layers were concentrated under reduced pressure, and the resultant red/black solid purified by flash column chromatography (silica gel; petroleum ether/ethyl acetate, 4:1). After evaporation of the solvent, the residue was dissolved in diethyl ether (3 × 20 mL) with the solvent being removed under reduced pressure after each addition. The solid was washed with petroleum ether (2 × 5 mL) and dried under vacuum to give the desired product as a red/purple solid (1.01 g, 55%). ^{1}H NMR ($CDCl_3$, 300 MHz): δ = 8.78 (d, ^3J = 8.1 Hz, 2 H, H$^{5'}$ and H$^{8'}$), 7.98 (br. s, 2 H, H^3 and H^5), 7.94 (dd, ^3J = 8.1, ^4J = 1.2 Hz, 1 H, H$^{1'}$), 7.90 (dd, ^3J = 8.4, ^4J = 1.2 Hz, 1 H, H$^{4'}$), 7.86 (s, 1 H, H$^{10'}$), 7.79 (ddd, ^3J = 8.4 and 6.9, ^4J = 1.5 Hz, 1 H, H$^{7'}$), 7.74–7.66 (m, 2 H, H$^{3'}$ and H$^{6'}$), 7.53 (ddd, ^3J = 8.1 and 7.8, ^4J = 1.2 Hz, 1 H, H$^{2'}$), 6.74 (d, ^3J = 4.2 Hz, 2 H, H^1 and H^7) and 6.46, (dd, ^3J = 3.9 and 0.9 Hz, 2 H, H^2 and H^6) ppm. ^{13}C NMR ($CDCl_3$, 100 MHz): δ = 146.05 (1 C), 144.74 (1 C), 136.34 (1 C), 131.43 (1 C), 131.40 (1 C), 131.01 (1 C), 130.45 (1 C), 130.35 (1 C), 129.86 (1 C), 129.50 (1 C), 129.36 (1 C), 128.27 (1 C), 127.54 (1 C), 127.47 (1 C), 127.29 (2 C), 122.91 (1 C), 122.87 (1 C), 118.77 (1 C) ppm. ^{11}B NMR ($CDCl_3$, 128 MHz): δ = –0.537 (t, $J_{B\text{-}F}$ = 27.08 Hz) ppm. ^{19}F NMR ([D$_6$]DMSO, 370 MHz): δ = –141.613 (dq, $J_{F\text{-}F}$ = 99.04, $J_{F\text{-}B}$ = 30.91 and 31.58 Hz) ppm. MS (EI): *m*/*z* = 368 [M]. HRMS (EI): calcd. for [$C_{23}H_{15}BF_2N_2$] 368.12963; found 368.13005 [M]. $C_{23}H_{15}BF_2N_2$ (368.2): calcd. C 75.03, H 4.11, N 7.60; found C 75.02, H 4.41, N 7.29. TLC (silica): R_f = 0.51 in petroleum ether/ethyl acetate, 4:1. M.p. 246–249 °C.

Acknowledgments

We thank the Engineering and Physical Sciences Research Council (EPSRC) (EP/G04094X/1) and the Newcastle University for financial support of this work.

[1] M. A. Haidekker, E. A. Theodorakis, *Org. Biomol. Chem.* **2007**, *5*, 1669–1678.
[2] a) J. Lu, C. L. Liotta, C. A. Eckert, *J. Phys. Chem. A* **2003**, *107*, 3995–4000; b) C. E. Kung, J. K. Reed, *Biochemistry* **1986**, *25*, 6114–6121; c) M. Lang, A. A. Dadali, H. G. Drickamer, *Chem. Phys. Lett.* **1993**, *214*, 10–17; d) K. I. Gutkowski, M. L. Japar, P. F. Aramendia, *Chem. Phys. Lett.* **2006**, *426*, 329–333.
[3] B. D. Allen, A. C. Benniston, A. Harriman, J. P. Rostron, C. F. Yu, *Phys. Chem. Chem. Phys.* **2005**, *7*, 3035–3040.
[4] V. I. Stsiapura, A. A. Maskevich, V. A. Kuzmitsky, V. N. Uversky, I. M. Kuznetsova, K. K. Turoverov, *J. Phys. Chem. B* **2008**, *112*, 15893–15902.
[5] a) M. A. Haidekker, D. Lichlyter, J. M. Ben, C. A. Grimes, *Sens. Lett.* **2006**, *4*, 257–261; b) C. Damas, M. Adibnejad, A. Benjelloun, A. Brembilla, M. C. Carré, M. L. Viriot, P. Lochon, *Colloid Polym. Sci.* **1997**, *275*, 364–371.
[6] V. I. Stsiapura, A. A. Maskevich, V. A. Kuzmitsky, V. N. Uversky, I. M. Kuznetsova, K. K. Turoverov, *J. Phys. Chem. B* **2008**, *112*, 15893–15902.
[7] a) I. Leray, B. Valeur, *Eur. J. Inorg. Chem.* **2009**, 3525–3535; b) K. Waich, T. Mayr, I. Klimart, *Talanta* **2008**, *77*, 66–72; c) P. D. Selid, H. Y. Xu, E. M. Collins, M. S. Face-Collins, J. X. Zhao, *Sensors* **2009**, *9*, 5446–5459.
[8] a) W. J. Akers, M. A. Haidekker, *J. Biomech. Eng.* **2005**, *127*, 450–454; b) A. Paul, A. Samanta, *J. Phys. Chem. B* **2008**, *112*, 16626–16632.
[9] M. E. Nipper, S. Majd, M. Mayer, J. C. M. Lee, E. A. Theodorakis, M. A. Haidekker, *Biochim. Biophys. Acta Biomembr.* **2008**, *1778*, 1148–1153.
[10] a) M. K. Kuimova, G. Yahioglu, J. A. Levitt, K. Suhling, *J. Am. Chem. Soc.* **2008**, *130*, 6672–6673; b) G. Hungerford, A. Allison, D. McLoskey, M. K. Kuimova, G. Yagioglu, K. Suhling, *J. Phys. Chem. B* **2009**, *113*, 12067–12074.
[11] M. A. H. Alamiry, A. C. Benniston, G. Copley, K. J. Elliott, A. Harriman, B. Stewart, Y.-G. Zhi, *Chem. Mater.* **2008**, *20*, 4024–4032.
[12] H. L. Kee, C. Kirmaier, L. Yu, P. Thamyongkit, W. J. Youngblood, M. E. Calder, L. Ramos, B. C. Noll, D. F. Bocian, W. R. Scheidt, R. R. Birge, J. L. Lindsey, D. Holten, *J. Phys. Chem. B* **2005**, *109*, 20433–20443.
[13] A. D. Buckingham, T. Schaefer, W. G. Scheider, *J. Chem. Phys.* **1960**, *32*, 1227–1233.
[14] R. Ziessel, C. Goze, G. Ulrich, M. Céarui, P. Retailleau, A. Harriman, J. P. Rostron, *Chem. Eur. J.* **2005**, *11*, 7366–7378.
[15] R. Y. Lai, A. J. Bard, *J. Phys. Chem. B* **2003**, *107*, 5036–5042.
[16] S. J. Strickler, R. A. Berg, *J. Chem. Phys.* **1962**, *37*, 814–822.
[17] A. C. Benniston, G. Copley, *Phys. Chem. Chem. Phys.* **2009**, *11*, 4124–4131.
[18] a) T. Rohand, J. Lycoops, S. Smout, E. Braeken, M. Sliwa, M. Van der Auweraer, W. Dehaen, W. M. De Borggraeve, N. Boens, *Photochem. Photobiol. Sci.* **2007**, *6*, 1061–1066; b) W.

Qin, T. Rohand, M. Baruah, A. Stefan, M. Van der Auweraer, W. Dehaen, N. Boens, *Chem. Phys. Lett.* **2006**, *420*, 562–568.
[19] a) W. Qin, M. Baruah, M. Van der Auweraer, F. C. De Schryver, N. Boens, *J. Phys. Chem. A* **2005**, *109*, 7371–7384; b) W. Qin, M. Baruah, A. Stefan, M. Van der Auweraer, N. Boens, *ChemPhysChem* **2005**, *6*, 2343–2351.
[20] B. Baggi, *Int. Rev. Phys. Chem.* **1987**, *6*, 1–33.
[21] a) J. Petravic, J. Delhommelle, *J. Chem. Phys.* **2005**, *122*, 234509; b) F. Gutman, L. M. Simmons, *J. Appl. Phys.* **1952**, *23*, 977–978.
[22] D. Ben-Amotz, C. B. Harris, *J. Chem. Phys.* **1987**, *86*, 4856–4870.
[23] R. Englman, J. Jortner, *Mol. Phys.* **1970**, *18*, 145–164.
[24] A. Gilbert, J. Baggott, *Essentials of Molecular Photochemistry*, Blackwell Scientific Publications, Oxford, **1991**.
[25] a) A. D. Osborne, *J. Chem. Soc. Faraday Trans. 2* **1980**, *76*, 1638–1645; b) J. A. B. Ferreira, S. M. B. Costa, L. F. V. Ferreira, *J. Phys. Chem. A* **2000**, *104*, 11909–11917.
[26] a) D. Ben-Amotz, C. B. Harris, *J. Chem. Phys.* **1987**, *86*, 4856–4870; b) D. Ben-Amotz, C. B. Harris, *J. Chem. Phys.* **1987**, *86*, 5433–5440.
[27] A. Harriman, L. J. Mallon, G. Ulrich, R. Ziessel, *ChemPhysChem* **2007**, *8*, 1207–1214.
[28] J. A. Riddick, W. B. Bunger, T. K. Sakano, *Organic Solvents*, 4th ed., Wiley-Interscience, New York, **1986**.

Received: October 6, 2009
Published Online: December 8, 2009

